Journal of proteome research

Article

pubs.acs.org/jpr

Proteomic Study of the Microdissected Aortic Media in Human Thoracic Aortic Aneurysms

Muge Serhatli,[†] Kemal Baysal,[‡] Ceyda Acilan,[†] Eylem Tuncer,[§] Seldag Bekpinar,[∥] and Ahmet Tarik Baykal*,[⊥]

[†]TUBITAK-Marmara Research Center, Genetic Engineering and Biotechnology Institute, 41470 Gebze, Kocaeli, Turkey

[‡]Dokuz Eylul University, Medical Faculty, Department of Biochemistry Inciralti, 35340 Izmir, Turkey

[§]Republic of Turkey Health Ministry, Kartal Kosuyolu Education and Research Hospital, 34846 Istanbul, Turkey

[∥]Department of Biochemistry, Istanbul Medical Faculty, Istanbul University, Capa, Istanbul 34093, Turkey

[⊥]Istanbul Medipol University, Department of Medical Biochemistry, School of Medicine, Ataturk Bulvari No:27, 34083 Unkapani, Fatih-Istanbul, Turkey

Supporting Information

ABSTRACT: Aortic aneurysm is a complex multifactorial disease, and its molecular mechanism is not understood. In thoracic aortic aneurysm (TAA), the expansion of the aortic wall is lead by extracellular matrix (ECM) degeneration in the medial layer, which leads to weakening of the aortic wall. This dilatation may end in rupture and—if untreated—death. The aortic media is composed of vascular smooth muscle cells (VSMCs) and proteins involved in aortic elasticity and distensibility. Delineating their functional and quantitative decrease is critical in elucidating the disease causing mechanisms as well as the development of new preventive therapies. Laser microdissection (LMD) is an advanced technology that enables the isolation of the desired portion of tissue or cells for proteomics analysis, while preserving their integrity. In our study, the aortic media layers of 36 TAA patients and 8 controls were dissected using LMD technology. The proteins isolated from these tissue samples were subjected to comparative proteomic analysis by nano-LC−MS/MS, which enabled the identification of 352 proteins in aortic media. Among these, 41 proteins were differentially expressed in the TAA group with respect to control group, and all were downregulated in the patients. Of these medial proteins, 25 are novel, and their association with TAA is reported for the first time in our study. Subsequent analysis of the data by ingenuity pathway analysis (IPA) shows that the majority of differentially expressed proteins were found to be cytoskeletal-associated proteins and components of the ECM which are critical in maintaining aortic integrity. Our results indicate that the protein expression profile in the aortic media from TAA patients differs significantly from controls. Further analysis of the mechanism points to markers of pathological ECM remodeling, which, in turn, affect VSMC cytosolic structure and architecture. In the future, the detailed investigation of the differentially expressed proteins may provide insight into the elucidation of the pathological processes underlying aneurysms.

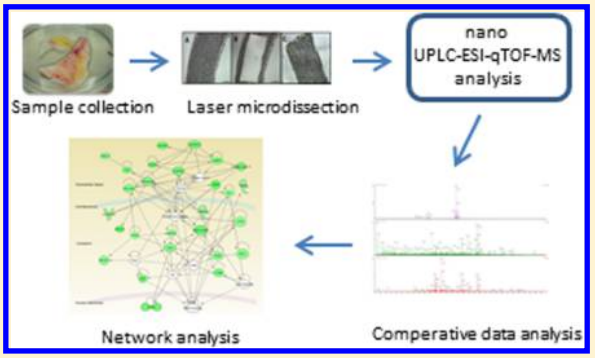

KEYWORDS: *thoracic aortic aneurysm, laser capture microdissection, label-free proteomics, protein expression, vascular smooth muscle*

INTRODUCTION

Aortic aneurysm is defined as a localized dilatation of the vessel reaching over >50% of its normal diameter, and the process includes all layers of the vessel.[1] Aneurysms can be located in the abdominal or thoracic segments of the aorta, presenting with different aetiopathologies. TAAs may have a genetic origin and present as syndromic or nonsyndromic diseases; they may also be observed spontaneously.[2] The prevalence of TAA is about one-third of that of AAA.[3] The structural heterogeneity of thoracic and abdominal aortas may contribute to the differences observed in the pathogenesis of AAA and TAA. The thoracic aorta has a thinner intima, thicker media, and more medial elastic lamina fibers than those of the abdominal aorta. The thoracic aorta has significantly higher elastin and collagen content.[4] Therefore, medial degeneration is qualitatively and quantitatively much greater in TAA patients.

In TAA, extensive extracellular matrix (ECM) degeneration leads to weakening and local dilatation of the aortic wall, potentially giving rise to aortic dissection or rupture. The microscopic findings in TAAs reflect loss of medial VSMCs, fragmentation, and depletion of elastic fibers and the accumulation of semimucoid ground substance and cysts,

Special Issue: Proteomics of Human Diseases: Pathogenesis, Diagnosis, Prognosis, and Treatment

Received: June 29, 2014

   dx.doi.org/10.1021/pr5006586 | J. Proteome Res. XXXX, XXX, XXX−XXX

termed medial degeneration.[5−8] Because aneurysm is a degenerative disease of the aortic media, a cohesive understanding of the complex structure and function in this vascular layer is necessary for the elucidation the pathogenesis of TAA and, ultimately, developing therapeutic modalities to prevent this disease.

The aortic media is composed of elastic fibers and VSMC interconnected with collagen fibers, proteoglycan, glycosaminoglycan, and various adhesive proteins.[9] All of these elements are essential for imparting elasticity and tensile strength and forming structural interactions between ECM components and VSMC.[9] Recent findings in TAA, such as increased production of reactive oxygen species, increased matrix metalloproteinase expression, and activity and alterations in the TGF-β signaling pathway, point to VSMC as key mediators of the disease process and aortic media as the central location of critical pathological events.[9] Previous studies have focused on the association certain genes and proteins with aneurysm.[10−14] Change of protein expression is predictive of the organization and functionality in tissue. A comprehensive investigation of the aortic media encompassing all VSMC and the ECM proteins may provide a more robust data to elucidate the pathogenesis of TAA.

All proteins in a biological sample are derived from animal, plant, or microorganism, defined as "proteome", and are mainly characterized using mass spectrometry.[15,16] In proteomic studies, proteins are isolated from biological samples; after trypsinization, they are separated by HPLC and further analyzed by mass spectrometry. The development of new proteomic techniques allows the simultaneous measurements of hundreds of proteins.[17−20] Recent proteomics studies on aneurysms have used the vascular intima media layer or whole vascular tissue.[21−24] Because aneurysm is a degenerative disease of the aortic media, the examination of the changes in this vascular layer may give deeper insight regarding the pathology.

Laser microdissection (LMD) is an advanced technology that enables the isolation of the desired portion of tissue or tissue cells without destroying their functions and phenotypes, and the samples thus obtained are accessible for proteomics analysis.[25,26]

In this study, precisely delineated areas of the media from aortas were obtained by using LMD technology, and proteomics was carried out on these materials in patients with TAA and controls.

MATERIALS AND METHODS

Aortic Samples

The study was approved by the ethics committee of Kartal Koşuyolu, Advanced Training and Research Hospital. All patients gave informed consent (Ethical Committee report number: 23, dated 21-3-2008 and protocol number: 184-04). Patients who underwent surgical operations for TAA or coronary artery bypass grafting (CABG) in the same hospital were asked to participate in this study. Patients with Marfan syndrome and bicuspid aortic valve and tissue specimens with atherosclerosis or thrombosis were excluded from the study. Aortic segments were collected from 36 patients with TAA, undergoing surgical repair (25 males, 11 females). Nondiseased aortic tissue form CABG patients (6 males, 2 females) who had a negative personal history of TAA were used as controls. Detailed information regarding the samples is given in Table 1.

Table 1. Distribution of Patients and Controls According to Demographic Data

	TAA	control
sample no.	36	8
gender	25 ♂, 11 ♀	6 ♂, 2 ♀
age	59.5 ± 9	49.5 ± 9
aortic diameter (cm)	5.7 ± 1.16	

Frozen Tissue Sectioning

The tissues were procured immediately after surgery and cut into the size of ∼1 cm × 1 cm pieces. After frozen by embedding in optimum cutting temperature (OCT) medium at −20 °C, frozen tissues were attached to the specimen clamp of the cryostat and were allowed to equilibrate to the cryostat temperature (e.g., −15 to −20 °C) for ∼15 min. Serial sections (10 μm) were obtained by using a cryostat microtome (Leica CM1100, Leica, Wetzlar, Germany) at −20 °C and placed on polyethylene naphthalate (PEN)-coated slides (Leica, Deerfield, IL). Slides were placed on dry ice or kept in the cryostat at −20 °C until use in LMD.

Ethanol and Xylene Dehydration

Dehydration is a critical step to achieve optimal results with LMD procedure. After thawing, the slides were fixed in 75% ethanol and then rehydrated in distilled water (LC−MS grade). Dehydration was performed by the sequential immersion, respectively, into 75, 95, and 100% ethanol. The slides were incubated each solution for 30 s.[27] After clearing in xylene two times, slides were air-dried for 5 min. Within an hour after fixation, the medial layer of tissue was marked and cut with the LMD equipment.

Laser Microdissection and Protein Extraction

LMD (Leica LMD6000 Leica Microsystems, Germany) was used to obtain the medial layer. The edges of the media layer of tissue fixed on slides were marked microscopically and were cut out by UV laser (337 nm) (Figure 1). Samples were collected in the tube caps containing 75 μL of UPX solution (Universal Protein Extraction Kit (Expedeon, San Diego, CA)) and 5 μL of protease inhibitor cocktail (Sigma-Aldrich, Germany). Sample volumes were brought to 150 μL with UPX solution and were homogenized with an ultrasonic homogenizer (Bandelin, Sonopuls mini 20, Germany) and then centrifuged at 15 000g for 10 min. The protein concentrations in the supernatants were measured by NanoDrop ND-1000 spectrophotometer (Nano-Drop Technologies, Wilmington, DE).

Sample Preparation for Analysis

Samples were prepared for proteomic analysis by using the filter-aided sample preparation (FASP) method.[28,29] For this purpose, FASP Protein Digestion Kit (Expedeon) was used. This method combines in-gel and in-solution digestion of the proteins, preparing them for mass-spectrometry-based proteomics. Initially, 100 μg protein in 30 μL of UPX was placed on the 30 kDa spin filter and washed with 6 M urea-containing FASP buffer. The purpose of washing with this buffer was to remove the detrimental low-molecular-weight components. A second step was to open the disulfide bonds in proteins by treating with iodoacetamide (IAA). Finally, the proteins were digested with trypsin and the tryptic peptides were eluted. The concentrations of resulting peptides were measured by nanodrop, and they were further analyzed by mass spectrometry.

dx.doi.org/10.1021/pr5006586 | J. Proteome Res. XXXX, XXX, XXX−XXX

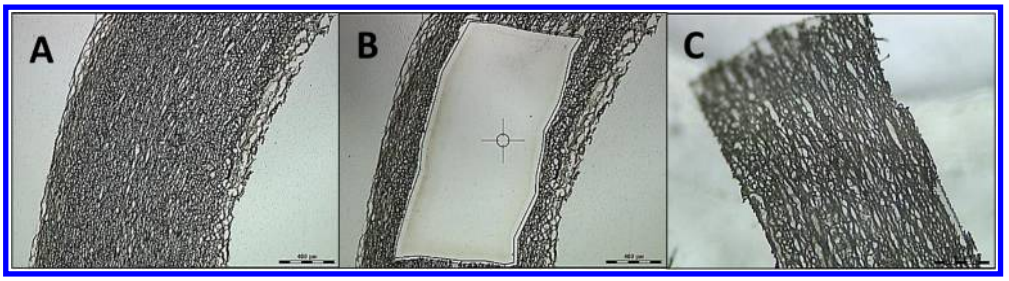

Figure 1. Aortic tissues were cut into 10 μm sections and were further dissected using a laser capture microdissection microscope. The images represent sections of (A) undissected, (B) dissected tissues, and (C) the specimen that was cut off. The combined samples of panel C was used for proteomics analysis.

LC–MS/MS Analysis

Tryptic peptides generated from aortic media layers were qualitatively and quantitatively analyzed with label-free nano-LC–MS/MS methodology. Peptide separation was performed on nanoACQUITY ultra pressure liquid chromatography (UPLC, Waters, Milford, MA). The columns were equilibrated with 97% mobile phase A (water, 0.1% formic acid) and 3% mobile phase B (acetonitrile, 0.1% formic acid). The column temperature was set to 45 °C. 500 ng of tryptic peptides in 5 μL volume was separated from the trap column (symmetry C18, 5 μm particle size, 180 μm i.d. × 20 mm, Waters) by gradient elution onto an analytical column (BEH C18, 1.7 μm particle size, 75 μm i.d. × 250 mm, Waters) with a linear gradient from 5 to 40% mobile phase B (acetonitrile, 0.1% formic acid) 300 nL/min flow rate over 90 min.

Peptide m/z measurement and sequencing were performed on a SYNAPT high-definition mass spectrometer with nanolock spray ion source (Waters). Parallel collision-induced dissociation (MSE) was carried out by operating the instrument at positive ion V mode, applying the MS and MS/MS functions over 1.5 s intervals with 6 V low collision energy and 15–40 V high collision energy ramp. Amino acid sequence was deduced according to the peptide mass to charge ratio (m/z) and the product ion information. To correct for the mass drift, the internal mass calibrant Glu-fibrinopeptide (500 pmol/μL) was infused every 45 s through the nanolockspray ion source at 300 nL/min flow rate. Peptide signal data between 50 and 1600 m/z values were collected.

LC–MS/MS Data Processing

Tandem mass spectra extraction, charge-state deconvolution, and deisotoping steps were processed with Protein Lynx Global Server v2.4 (Waters) and searched with the Identity^E algorithm against the *Homo sapiens* reviewed protein database from Uniprot (June 1, 2012, 25 899 entries). Identity^E was set up to search null assuming the digestion enzyme trypsin and searched with a fragment ion mass tolerance of 20 ppm and a parent ion tolerance of 10 ppm. The amino acid sequence of the internal standard (yeast enolase, Uniprot accession no. P00924) was included in the FASTA file of the database. The Apex3D data preparation parameters were set to 0.2 min chromatographic peak width, 10 000 MS TOF resolution, 150 counts for low energy threshold, 50 counts for elevated energy threshold, and 1200 counts for the intensity threshold. Databank search query was set to minimum three fragment ion matches per peptide; minimum seven fragment ion matches per protein; minimum one peptide matches per protein, and one missed cleavage. Carbamidomethyl-cysteine-fixed modification and acetyl N-TERM, deamidation of asparagine and glutamine, and oxidation of methionine variable modifications were set.

Progenesis LC–MS software V4.0 (nonlinear dynamics) software was used for the quantification of the protein expression changes. Normalization of the peptide expression is based on total ion intensity. After normalization, a PCA analysis was performed to assess the sample groups regarding outliers and similarities of the technical replicates of the same sample. None of the analysis from the sample set needed to be removed based on the PCA analysis. Power analysis was also performed for the data set, which shows whether the sample set has enough replicates to see real differences among sample groups. Chromatographic alignment, normalization calculation of peptide abundances, and expression changes were carried out, and an Excel file listing the normalized abundances of all identified proteins was generated. Similar proteins were grouped, and quantitative value is given for the one with the highest score. Protein quantitation is done with only the nonconflicting peptide features.

The acquired protein fold changes were used in the IPA analysis (version 8.5). The canonical pathways used to construct the protein–protein interaction map were generated with protein identifications having a p value <0.05 and greater than 40% expression change.

RESULTS

Before proteomics analysis, all tissue specimens were examined microscopically. Tissue sections from TAA were observed to be thinner and having a porous and irregular structure as compared with control tissues, indicating loss of ECM and tissue organization (Figure 2). Comparative proteome analysis of aortic media obtained from normal and thoracic aneurysmal aorta was performed by LC–MS/MS system (nanoACQUITY-UPLC) and an SYNAPT high-definition mass spectrometer with nanolockspray ion source (Waters). Proteins were qualitatively identified according to exact mass and retention

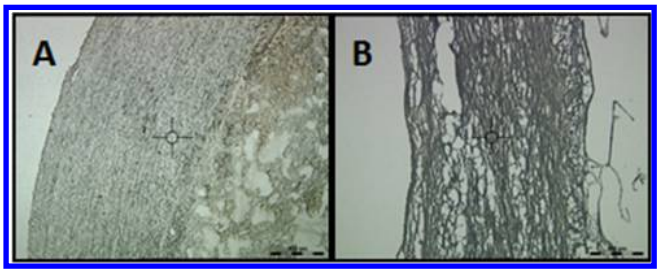

Figure 2. Morphology of aortic tissue obtained from either (A) control or (B) TAA patients. There was a drastic difference between the control (heart transplant tissue) and aneurysmal aorta, which contained acellular areas and appeared loose.

dx.doi.org/10.1021/pr5006586 | J. Proteome Res. XXXX, XXX, XXX–XXX

Table 2. PLGS Analysis of the Differentially Expressed Proteins in This Study[a]

accession	description	peptide count	peptides used for quantitation	score	Anova (p)[b]	fold	novel proteins[d]	average normalized abundances[c]	
								control	TAA
P35749	MYH11 myosin 11	323	1	1773.25	1.32×10^{-3}	2.18↓	–	433.01	198.50
P35580-2	MYH10isoform 2 of myosin	269	5	1465.97	0.04	1.58↓	–	1663.48	1052.02
P02751-5	FINC fibronectin	212	1	1114.87	8.06×10^{-3}	1.78↓	–	2189.04	1227.92
P98160	PGBM basement membrane specific heparan sulfate proteoglycan core protein	81	52	594.53	0.03	1.46↓	+	6.29×10^{4}	4.31×10^{4}
A5A3E0	POTEF POTE ankyrin domain family member F	102	5	490.45	0.04	1.50↓	+	1377.76	919.64
P07951-2	TPM2 isoform 2 of tropomyosin beta chain	79	4	488.72	0.04	1.60↓	+	6313.76	3941.20
P10909-2	CLUS isoform 2 of clusterin	66	41	355.46	0.04	1.43↓	–	4.09×10^{4}	2.87×10^{4}
P12110	CO6A2 collagen alpha 2 VI chain	49	13	316.87	0.02	1.90↓	+	2.33×10^{4}	1.22×10^{4}
Q562R1	ACTBL beta actin like protein 2	60	13	310.60	0.02	1.66↓	+	4.10×10^{4}	2.47×10^{4}
P55083	MFAP4 microfibril associated glycoprotein 4	46	23	261.01	0.02	1.69↓	–	3.75×10^{4}	2.22×10^{4}
P51888	PRELP prolargin	47	23	259.51	0.04	1.50↓	+	1.72×10^{4}	1.15×10^{4}
P0CG39	POTEJ POTE ankyrin domain family member J	63	2	258.00	0.04	2.05↓	+	2887.29	1411.61
P20774	MIME mimecan	48	29	251.80	0.05	1.49↓	–	2.35×10^{4}	1.57×10^{4}
P35609	ACTN2 alpha actinin 2	49	3	249.40	0.02	1.95↓	+	3.22×10^{4}	1.65×10^{4}
P68871	HBB hemoglobin subunit beta	43	10	220.18	3.09×10^{-3}	3.14↓	–	5.46×10^{4}	1.74×10^{4}
P69905	HBA hemoglobin subunit alpha	30	20	167.71	3.14×10^{-3}	2.65↓	–	3.68×10^{4}	1.39×10^{4}
Q9BYX7	ACTBM putative beta actin like protein 3	41	5	160.93	0.03	1.57↓	+	1491.10	951.50
O75369-5	FLNB isoform 5 of filamin B	28	3	141.46	9.31×10^{-3}	1.74↓	+	2705.55	1555.67
P17661	DESM desmin	31	4	133.70	1.52×10^{-3}	1.88↓	–	1388.02	738.69
P55268	LAMB2 laminin subunit beta 2	19	14	128.06	6.43×10^{-3}	1.84↓	–	1.29×10^{4}	7021.72
P06753	TPM3 tropomyosin alpha 3 chain	27	2	110.04	0.05	1.44↓	+	3281.67	2281.94
Q9UBX5	FBLN5 fibulin 5	23	7	98.75	0.04	1.58↓	+	1.44×10^{4}	9141.30
Q6PEY2	TBA3E tubulin alpha 3E chain	19	1	86.49	5.38×10^{-3}	2.66↓	+	1818.01	682.74
P63104	1433Z 14 3 3 protein zeta delta	18	5	78.16	0.03	1.58↓	–	758.16	480.26
P02746	C1QB complement C1q subcomponent subunit B	15	6	72.57	0.04	1.54↓	+	5764.89	3736.74
P39060-1	COIA1 isoform 2 of collagen alpha 1 XVIII chain	11	1	70.79	0.04	1.60↓	+	1566.53	977.73
P08294	SODE extracellular superoxide dismutase Cu Zn	14	7	69.98	0.04	1.50↓	–	5161.82	3442.96
P02671-2	FIBA isoform 2 of fibrinogen alpha chain	12	9	67.97	0.02	1.74↓	+	5417.73	3108.68
O15230	LAMA5 laminin subunit alpha 5	10	6	55.59	0.03	1.85↓	–	3190.22	1720.13
P31946-2	1433B isoform short of 14 3 3 protein beta alpha	11	2	52.06	7.38×10^{-3}	1.90↓	–	1170.55	617.02
Q96AC1-3	FERM2 isoform 3 of fermitin family homologue 2	7	1	35.61	0.01	1.89↓	+	4811.08	2549.86
P11047	LAMC1 laminin subunit gamma 1	7	4	35.55	0.02	1.76↓	+	4163.91	2367.09
P35625	TIMP3 metalloproteinase inhibitor 3	2	1	29.20	6.56×10^{-3}	2.13↓	–	686.90	322.72
Q96A32	MLRS myosin regulatory light chain 2 skeletal muscle isoform	6	3	24.27	0.04	1.57↓	+	904.09	576.17
O15498	YKT6 synaptobrevin homologue YKT6	4	1	22.06	0.03	1.95↓	+	882.01	451.58
Q08380	LG3BP galectin 3 binding protein	1	1	14.80	0.02	1.69↓	–	554.67	327.57
Q12899	TRI26tripartite motif containing protein 26	1	1	14.14	7.31×10^{-4}	1.68↓	+	8347.55	4962.00
P18754	RCC1 regulator of chromosome condensation	1	1	13.64	0.04	1.55↓	+	7762.74	5012.43
Q96PX9	PKH4B pleckstrin homology domain containing family G member 4B	1	1	13.22	0.02	1.67↓	+	8087.22	4851.61
P49758-6	RGS6 isoform 6 of Regulator of G protein signaling 6	1	1	7.13	0.02	1.45↓	+	228.10	157.16
Q14247	SRC8 Src substrate cortactin	1	1	6.87	0.02	1.46↓	+	557.64	382.47
Q5VWW1-2	C1QL3 isoform 2 of complement C1q like protein 3	1	1	6.79	0.03	1.53↓	+	644.34	422.46

dx.doi.org/10.1021/pr5006586 | J. Proteome Res. XXXX, XXX, XXX–XXX

Table 2. continued

[a]Accession number, protein description, number of identified peptide, and abundance of identified proteins are listed. [b]$p < 0.05$. [c]With respect to control group by using ($p \leq 0.05$) and by setting to 40% cut off (up- or downregulated more). [d]Novel nonassociated proteins of aneurysms in this study are shown +.

Table 3. Differentially Expressed Proteins in This Study and a Comparison with the Literature

our results	protein expression	literature	comment/reference
Proteins Previously Shown to Be Associated with TAA			
myosin 11 (MYH11)	↓ × 2.18		MYH gene mutations are a cause of familial aortic aneurysms[38,39]
myosin 10 (MYH10)	↓ × 1.58	↑ × 2	increased in Marfan patients[23]
hemoglobin alpha subunit (HBA)	↓ × 2.65	↓ × 2.45	decreased in TAA patients (intima-media layers)[37]
hemoglobin beta subunit (HBB)	↓ × 3.14	↓ × 3.06	decreased in TAA patients (intima-media layers)[37]
laminin beta-2 subunit	↓ × 1.78	↑	increased gene expression[40]
14−3−3 protein beta/alpha (1433B)	↓ × 1.89	↑ × 1.43	increased in TAA patients (intima-media layers)[37]
desmin	↓ × 1.87	↓	decreased in TAA patients[41]
Proteins Previously Shown to Be Associated with AAA			
clusterin	↓ × 1.43	↓	decreased in AAA patients serum[42]
laminin alpha-5 subunit	↓ × 1.85	↓	decreased in AAA patients patients (whole tissue)[31]
galectin-3 binding protein	↓ × 1.69	↓	decreased in AAA patients patients (whole tissue)[31]
Proteins Previously Shown to Be Associated with AAA and TAA			
fibronectin (FINC)	↓ × 1.78	↓, ↓	decreased in Marfan patients,[43] decreased in AAA patients patients (whole tissue)[31]
mimecan/osteoglisin	↓ × 1.49	↓, ↑	decreased calcified AAA tissues patients (whole tissue),[44] increased gene expression in TAA patients[45]
14−3−3 protein zeta/delta	↓ × 1.57	↑ × 1.12	increased in TAA patients (intima-media layers),[37] referans gen for AAA[46]
tissue inhibitor of metalloproteinase-3	↓ × 2.12	↓, ↑	decreased gene expression in TAA,[40] increased gene expression in AAA[47]
microfibril-associated glycoprotein 4	↓ × 1.68	↓× 1.20, ↓, ↑ × 2.08	decreased in TAA patients (intima-media layers),[37] decreased in AAA patients (whole tissue),[48] increased in Marfan/BAV patients[23]
extracellular superoxide dismutase Cu−Zn	↓ × 1.49	↓, ↑ × 1.94	decreased in TAA BAV patients (whole tissue),[49] increased in AAA patients plasma[50]

time (EMRT). Relative abundance of these identified proteins was evaluated with respect to control by using the Protein Lynx Global SERVER (PLGS v2.4, Waters) expression module. The threshold for statistical significance for a particular protein was considered to be 40% expression change between the patient and control samples.

A total of 352 proteins were identified in aortic media from TAA patients and controls. Among them, 41 proteins were found to be significantly different in aneurysm group with respect to the control group, and all were downregulated. These proteins are shown in Table 2 with the accession numbers, descriptions, peptide counts, the number of peptides used for quantization, and confidence scores.

Of these, 16 proteins were previously described to be associated with aneurysm (Table 3). Proteins previously shown to be associated with TAA included desmin, myosin 11, myosin 10, hemoglobin beta subunit, hemoglobin alpha subunit, laminin subunit beta-2, and 14−3−3 protein beta/alpha. Those previously shown to be associated with AAA were clusterin, laminin alpha-5 subunit, and galectin-3 binding protein. Proteins associated with both AAA and TAA were extracellular superoxide dismutase Cu−Zn, microfibril-associated glycoprotein 4, mimecan/osteoglisin, 14−3−3 protein zeta/delta, tissue inhibitor of metalloproteinase-3, and fibronectin. The remaining 25 proteins were not reported to be associated with aneurysm previously and are novel findings of this study. These proteins are POTE ankyrin domain family member F, perlecan (basement membrane-specific heparan sulfate proteoglycan core protein), POTE ankyrin domain family member J, beta actin like protein 2, putative beta actin like protein 3, collagen alpha 2 VI chain, alpha actinin 2, tropomyosin alpha 3 chain, filamin B, fibulin 5, tubulin alpha 3E chain, complement C1q subcomponent subunit B, collagen alpha 1 XVIII chain, fibrinogen alpha chain, fermitin family homologue 2, laminin subunit gamma 1, myosin regulatory light chain 2 skeletal muscle isoform, synaptobrevin homologue, tripartite motif containing protein 26, pleckstrin homology domain containing family G member 4B, regulator of chromosome condensation, regulator of G protein signaling 6, Src substrate cortactin, complement C1q like protein 3, and tropomyosin beta chain.

To understand how these differentially expressed proteins are associated with each other, as well as other signal transduction pathways, the data were further analyzed using Ingenuity Pathway Analysis (IPA version 8.5) software (Figures 3 and 4). IPA is a knowledge database relying on published literature related to protein function, localization, relevant interactions and biological mechanisms. Accordingly, based on their structure and function, most of the differentially expressed proteins were related to connective tissue disorders, cell signaling and organization (Table 4). Score indicates the log of the probability of network eligible proteins appearing in the network by random chance. High-score value shows low probability of randomness and high reliability. Score ≥2 is accepted to be significant. Twenty-one proteins were merged strongly in a single network with a score of 53 (Table 5). The second network involving in 13 proteins had score of 29 in our analysis.

dx.doi.org/10.1021/pr5006586 | J. Proteome Res. XXXX, XXX, XXX−XXX

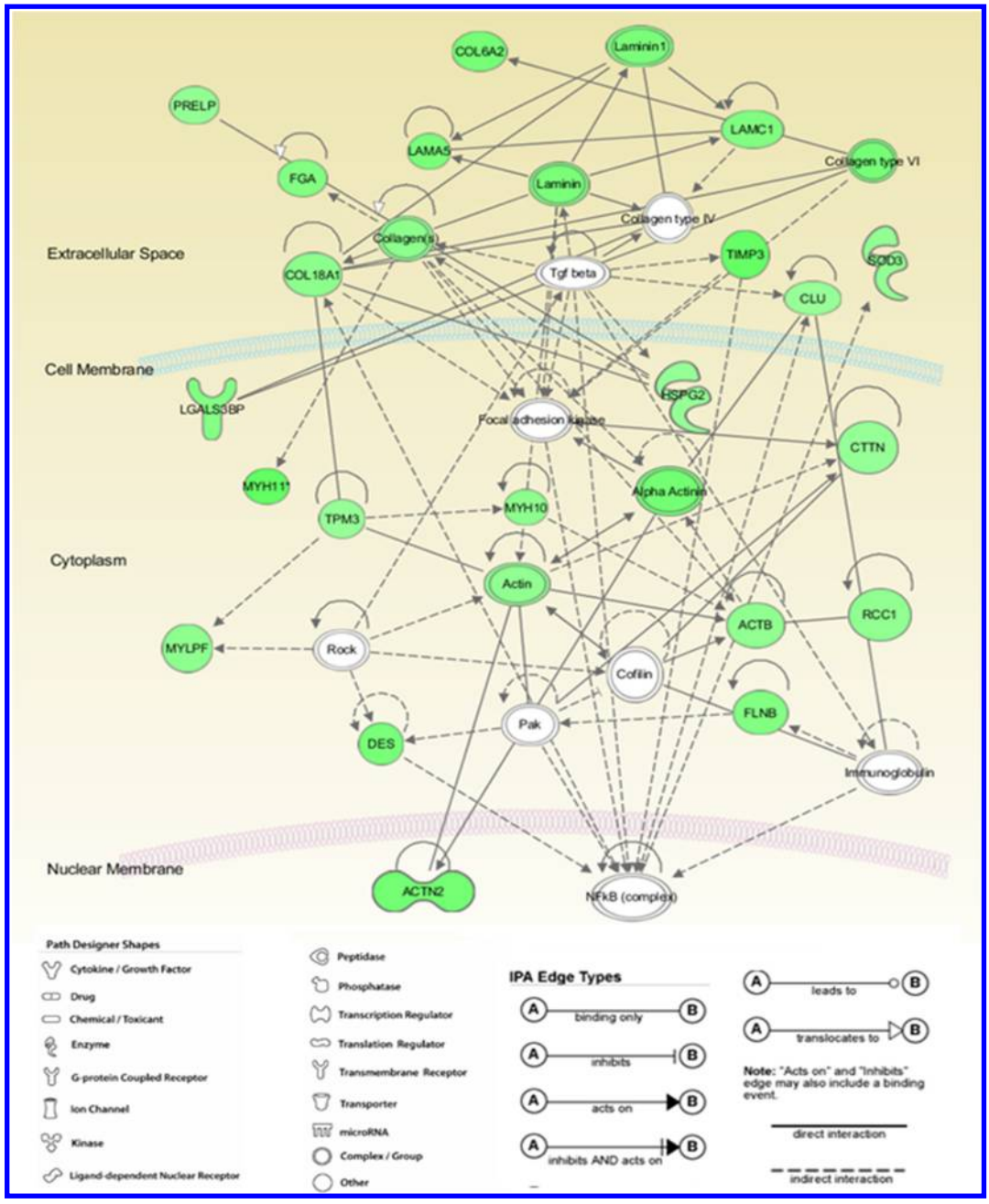

Figure 3. Most high-scored network (Network 1) generated by IPA (ingenuity pathway analysis). The network with the highest score is shown on the graph (IPA score: 53). The relationship between the differentially regulated proteins was studied using IPA software. The colored nodes indicate proteins that were identified in this proteomic analysis, while the colorless nodes are added by the program. Green color denotes upregulation, while red denotes downregulation. The intensity of the color correlates with the fold change. The key for the shape of the nodes, the line types, and the edge types are given below the network.

DISCUSSION

TAA is a virulent, potentially lethal, but predominantly silent disease. TAA has often been diagnosed when dissection and rupture occurs in patients or incidentally during screening tests made for other purposes. Therefore, efforts to understand the mechanism and improve the diagnosis of disease are of great importance. The precise pathogenesis of medial degeneration that provides the anatomic background for dissection and rupture is not fully understood. The detailed characterization of differentially expressed proteins in medial layers of patients with TAA can help in elucidating the molecular mechanisms of aneurysm. Therefore, we planned to investigate all proteins in the aortic media layer from patients with TAA and compared them with control samples at the proteome level. We employed LMD technology that enabled the isolation of a sharply delineated area in the tissue, with no contamination from the adjacent adventitia or intima. We examined all proteins present in these materials by proteome analysis. Our aim was to identify the proteins related to pathological remodeling of aortic media in TAA.

In our proteomic analysis, we identified 352 proteins in aortic media layers from TAA patients and controls. Of these proteins, 41 were found to be differentially expressed between these groups and all were downregulated in TAA patients.

dx.doi.org/10.1021/pr5006586 | J. Proteome Res. XXXX, XXX, XXX−XXX

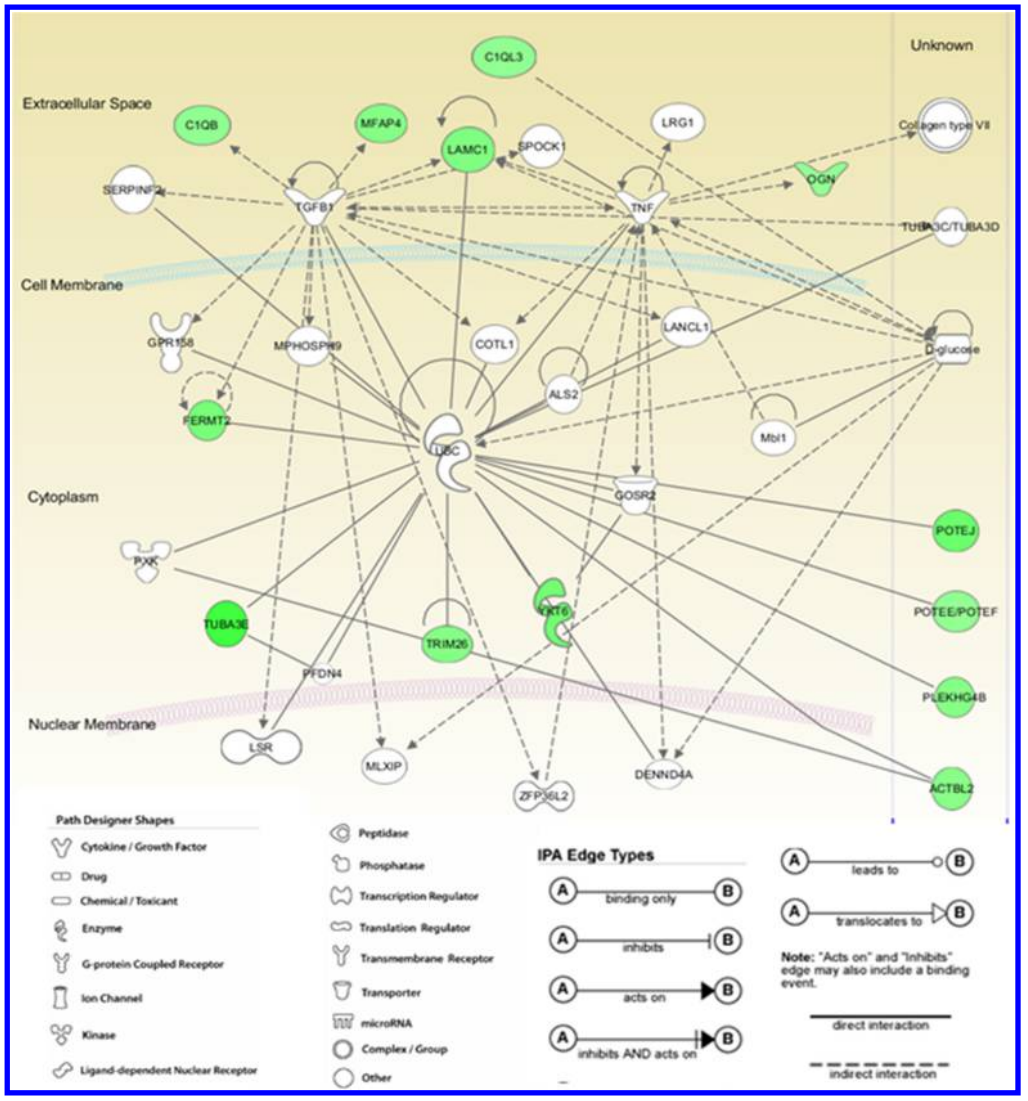

Figure 4. Second high-scored network (Network 1) generated by IPA (ingenuity pathway analysis). Second most high-scored network is shown on the graph (IPA score: 29). The color codes and shapes are the same as explained for Figure 3.

Twenty-five of these proteins were demonstrated for the first time to be uniquely involved with TAA patients in our study. Among these novel proteins, TBA3E and POTEJ have the highest change in amount, and their levels decreased 2.66- and 2.06-fold, respectively. These proteins are involved in cellular and developmental processes, RGS6 is a protein reported to be related to apoptosis and ROS production.[30] Both processes also actively involved during aneurysm formation processes.

Thirteen of downregulated proteins in aortic media of TAA patients were associated with ECM integrity. These are collagen alpha 2 VI chain, collagen alpha 1 XVIII chain, microfibril-associated glycoprotein 4, laminin subunit beta-2, laminin alpha-5 subunit, galectin-3 binding protein, laminin subunit gamma 1, fibronectin, fibulin 5, perlecan (basement membrane-specific heparan sulfate proteoglycan core protein), mimecan/osteoglisin, fermitin family homologue 2, and tissue inhibitor of metalloproteinase-3.

Laminins, a family of ECM glycoproteins, are implicated in a wide variety of biological process including cell adhesion, differentiation, migration, and signaling.[31] The observed decreases in fibronectin, laminin subunit beta-2, laminin alpha-5 subunit, and laminin subunit gamma 1 in the media are compatible with ECM degeneration in patients with TAA.

Mature VSMCs normally express a group of cytosolic and membrane proteins necessary for contractile function[32] but show phenotypic plasticity, being able to undergo a transition from a quiescent, contractile state to a synthetic, proliferative form.[33] However, various pathological conditions such as atherosclerosis, restenosis, and hypertension have been shown to change them to a synthetic phenotype.[34] Such phenotypic modulation has also been reported in aortic aneurysms.[35]

Deficiencies of cytoskeletal proteins may lead to impaired vessel wall remodeling and thus alter the organizational, synthetic, and contractile capability of SMCs and promote aneurysm.[9] In this study, 12 proteins that are known to interact with the cytoskeleton were found to be decreased in the TAA group. These are tubulin alpha 3E chain, desmin, beta actin like protein 2, putative beta actin like protein 3, alpha actinin 2, tropomyosin alpha 3 chain, myosin regulatory light chain 2 skeletal muscle isoform, tropomyosin beta chain, myosin 11, myosin 10, filamin B, and Src substrate cortactin.

Myosins are actin-binding proteins that have contractile properties. They have a pivotal role in the control of cell

dx.doi.org/10.1021/pr5006586 | J. Proteome Res. XXXX, XXX, XXX−XXX

Table 4. Top Biological Functions in Differentially Expressed Proteins Based on Ingenuity Pathway Analysis

diseases and disorders	*p* value	no. molecule
connective tissue disorders	8.81×10^{-6} to 7.78×10^{-3}	18
developmental disorders	8.81×10^{-6} to 9.12×10^{-3}	15
hereditary disorders	8.81×10^{-6} to 9.12×10^{-3}	17
molecular and cellular functions	***p* value**	**no. molecule**
cellular movement	6.12×10^{-7} to 9.12×10^{-3}	17
cell-to-cell signaling and interaction	1.63×10^{-6} to 9.12×10^{-3}	19
cellular assembly and organization	1.63×10^{-6} to 9.12×10^{-3}	21
cellular function and maintenance	1.70×10^{-6} to 9.12×10^{-3}	18
cell morphology	1.70×10^{-6} to 9.12×10^{-3}	19
physiological system development and function	***p* value**	**no. molecule**
cardiovascular system development and function	3.72×10^{-7} to 9.65×10^{-3}	16
organ morphology	3.72×10^{-7} to 9.12×10^{-3}	17
tissue morphology	6.12×10^{-7} to 9.12×10^{-3}	14
tissue development	1.63×10^{-6} to 9.12×10^{-3}	21
embryonic development	2.85×10^{-6} to 9.12×10^{-3}	16

adhesion and tissue architecture. The proteins given above are involved in the contractile machinery of VSMCs, and the decrease in their expression correlates with the switch to a synthetic state of these cells observed in TAA.[36]

Hypoxia and increased oxidative stress also probably contribute to medial degeneration.[21] In this study, downregulated hemoglobin beta subunit, hemoglobin alpha subunit, extracellular superoxide dismutase Cu−Zn, and clusterin in TAA patients may be associated with defective oxygen transport and antioxidant capacity.

In addition to being active in oxygen transport, hemoglobin beta subunit has been shown by UniProt protein databases (GO:0050880, June 11, 2014, version 130) to participate in the regulation of blood vessels size.

Kjellqvist and colleagues[37] have reported a decrease in hemoglobin beta subunit and hemoglobin alpha subunit in TAA patients in a study using matrix-assisted laser dissorption ionization (MALDI); our findings corroborate and confirm the results. In addition, a reduction in some proteins likely to be involved in cell signaling was identified in TAA patients. These proteins are 14−3−3 protein beta/alpha, 14−3−3 protein zeta/delta, regulator of G protein signaling 6, and complement C1q like protein 3. In a proteomic study in Marfan patients with aneurysms using 2D-DIGE and mass spectrometry, increased Myosin 10 and Filamin A but decreased hemoglobin alpha and beta subunits were reported in the media.[23]

Our results indicate that protein profiles of aortic media were significantly altered in TAA, which may contribute to the pathogenesis of the disease.

The networks generated by IPA analysis indicate that in our TAA patients downregulated proteins are involved in two major networks: (a) cardiovascular system development and function, organ morphology, cellular assembly, and organization and (b) proteins related to cell death and survival, hematological system development and function, and endocrine system disorders.

This study is particularly important not only because it explains the proteomic mechanisms of TAAs but also because it

Table 5. High-Scored Biological Networks Formed by Differentially Expressed Proteins Based on Ingenuity Pathway Analysis[a]

network ID	molecules in network	score	focus molecules	top functions
1	**ACTB**↓, actin, **ACTN2**↓, α-actinin, **CLU**↓, cofilin, **COL18A1**↓, **COL6A2**↓, collagen type VI, collagen(s), **CTTN**↓, **DES**↓, **FGA**↓, **FLNB**↓, focal adhesion kinase, **HSPG2**↓, immunoglobulin, **LAMA5**↓, **LAMC1**↓, laminin1, laminin, **LGALS3BP**↓, **MYH10**↓, **MYH11**↓, **MYLPF**↓, NFκB (complex), Pak, **PRELP**↓, **RCC1**↓, Rock, **SOD3**↓, Tgf beta, **TIMP3**↓, **TPM3**↓	53	21	cardiovascular system development and function, organ morphology, cellular assembly and organization
2	**ACTBL2**↓, ALS2, **C1QB**↓, **C1QL3**↓, collagen type VII, COTL1, D-glucose, DENND4A, **FERMT2**↓, GOSR2, GPR158, **LAMC1**↓, LANCL1, LRG1, LSR, Mbl1, **MFAP4**↓, MLXIP, MPHOSPH9, **OGN**↓, PFDN4, **PLEKHG4B**↓, **POTEE/POTEF**↓, **POTEJ**↓, PXK, SERPINF2, SPOCK1, TGFB1, TNF, **TRIM26**↓, TUBA3C/TUBA3D, **TUBA3E**↓, UBC, **YKT6**↓, ZFP36L2	29	13	cell death and survival, hematological system development and function, endocrine system disorders
3	Akt, ANGPTL1, Ap1, Cg, **COL21A1**↓, collagen, collagen Type I, ERK, estrogen receptor, **FBLN5**↓, **FERMT2**↓, fibrinogen, **FN1**↓, FOXN2, FSH, **HBB**↓, histone h3, Hsp90, insulin, integrin, Jnk, **LAMB2**↓, Mmp, P38 MAPK, PDGF BB, PI3K (complex), Pld, **RGS6**↓, SH3BP5L, Sos, TCR, TESK2, Vegf, **YWHAB**↓, **YWHAZ**↓	18	9	cellular movement, cardiovascular system development and function, cell morphology

[a]In this Table, proteins labeled in bold were identified as significantly differentially regulated and others were added by IPA for network analysis. A total of three networks was found with a score >2, which is considered to be significant. The top functions, number of focus molecules, and the score number for each network are given. Networks 1 and 2 are drawn in Supplemental Figures 3 and 4 in the Supporting Information.

dx.doi.org/10.1021/pr5006586 | J. Proteome Res. XXXX, XXX, XXX−XXX

is the first study focusing on and dissecting the medial aortic layer using LMD. Studying the tissue as a whole has the risk of masking differential changes in VSMC, which in addition to the medial ECM have been targeted in this study.

In conclusion, most proteins found to be decreased in the media layers of TAA patients are cytoskeleton-associated proteins and ECM components. Whether the observed protein expression changes are the cause or effect of TAA is currently unclear. Further investigation of proteins that are found to be associated with TAA in this study may provide benefit to the elucidation pathological process underlying aneurysm. Indeed, this study warrants further investigation of the differentially expressed proteins through immunoblotting and other methods.

■ ASSOCIATED CONTENT

Supporting Information

Peptide information and tissue raw data. This material is available free of charge via the Internet at http://pubs.acs.org.

■ AUTHOR INFORMATION

Corresponding Author

*Phone: +90-212-453-4926. Fax: +90-212-531-7555. E-mail: atbaykal@medipol.edu.tr.

Notes

The authors declare no competing financial interest.

■ ACKNOWLEDGMENTS

This work has been supported by The Research Fund of Istanbul University (project no. 11537), EU 7th Framework Program project; Fighting Aneurysmal Disease (Health-F2-2008-200647) and TUBITAK Marmara Research Center, Genetic Engineering and Biotechnology Institute.

■ REFERENCES

(1) Johnston, K. W.; Rutherford, R. B.; Tilson, M. D.; Shah, D. M.; Hollier, L.; Stanley, J. C. Suggested standards for reporting on arterial aneurysms. Subcommittee on Reporting Standards for Arterial Aneurysms, Ad Hoc Committee on Reporting Standards, Society for Vascular Surgery and North American Chapter, International Society for Cardiovascular Surgery. *J. Vasc. Surg.* **1991**, *13* (3), 452−458.

(2) Ince, H.; Nienaber, C. A. Granulocyte-colony-stimulating factor in acute myocardial infarction: future perspectives after FIRSTLINE-AMI and REVIVAL-2. *Nat. Clin. Pract. Cardiovasc. Med.* **2007**, *4* (Suppl 1), S114−S118.

(3) Kuivaniemi, H.; Platsoucas, C. D.; Tilson, M. D., 3rd Aortic aneurysms: an immune disease with a strong genetic component. *Circulation* **2008**, *117* (2), 242−252.

(4) Tonar, Z.; Witter, K.; Křížková, V.; Eberlová, L.; Kočová, J.; Moláček, J.; Houdek, K.; Kochová, P.; Vrzalová, J.; Topolčan, O. Stereological Tools for Quantitative Microscopy of the Aortic Wall with Focus on the Abdominal Aortic Aneurysm. In *Microscopy: Science, Technology, Applications and Education*; Méndez-Vilas, A.; Diaz, J., Eds.; Microscopy Book Series; Formatex Research Center: Badajoz, Spain, 2010; pp 926−935.

(5) Moritz, A. R. Medionecrosis Aortae Idiopathica Cystica. *Am. J. Pathol.* **1932**, *8* (6), 717−734.3.

(6) Niwa, K.; Perloff, J. K.; Bhuta, S. M.; Laks, H.; Drinkwater, D. C.; Child, J. S.; Miner, P. D. Structural abnormalities of great arterial walls in congenital heart disease: light and electron microscopic analyses. *Circulation* **2001**, *103* (3), 393−400.

(7) Marsalese, D. L.; Moodie, D. S.; Lytle, B. W.; Cosgrove, D. M.; Ratliff, N. B.; Goormastic, M.; Kovacs, A. Cystic medial necrosis of the aorta in patients without Marfan's syndrome: surgical outcome and long-term follow-up. *J. Am. Coll. Cardiol.* **1990**, *16* (1), 68−73.

(8) de Sa, M.; Moshkovitz, Y.; Butany, J.; David, T. E. Histologic abnormalities of the ascending aorta and pulmonary trunk in patients with bicuspid aortic valve disease: clinical relevance to the ross procedure. *J. Thorac. Cardiovasc. Surg.* **1999**, *118* (4), 588−594.

(9) Wu, D.; Shen, Y. H.; Russell, L.; Coselli, J. S.; LeMaire, S. A. Molecular mechanisms of thoracic aortic dissection. *J. Surg. Res.* **2013**, *184* (2), 907−924.

(10) Milewicz, D. M.; Guo, D. C.; Tran-Fadulu, V.; Lafont, A. L.; Papke, C. L.; Inamoto, S.; Kwartler, C. S.; Pannu, H. Genetic basis of thoracic aortic aneurysms and dissections: focus on smooth muscle cell contractile dysfunction. *Annu. Rev. Genomics Hum. Genet.* **2008**, *9*, 283−302.

(11) Boileau, C.; Guo, D. C.; Hanna, N.; Regalado, E. S.; Detaint, D.; Gong, L.; Varret, M.; Prakash, S. K.; Li, A. H.; d'Indy, H.; Braverman, A. C.; Grandchamp, B.; Kwartler, C. S.; Gouya, L.; Santos-Cortez, R. L.; Abifadel, M.; Leal, S. M.; Muti, C.; Shendure, J.; Gross, M. S.; Rieder, M. J.; Vahanian, A.; Nickerson, D. A.; Michel, J. B.; Jondeau, G.; Milewicz, D. M. TGFB2 mutations cause familial thoracic aortic aneurysms and dissections associated with mild systemic features of Marfan syndrome. *Nat. Genet.* **2012**, *44*, 916−921.

(12) Vaughan, C. J.; Casey, M.; He, J.; Veugelers, M.; Henderson, K.; Guo, D.; Campagna, R.; Roman, M. J.; Milewicz, D. M.; Devereux, R. B.; Basson, C. T. Identification of a chromosome 11q23.2-q24 locus for familial aortic aneurysm disease, a genetically heterogeneous disorder. *Circulation* **2001**, *103* (20), 2469−2475.

(13) Guo, D.; Hasham, S.; Kuang, S. Q.; Vaughan, C. J.; Boerwinkle, E.; Chen, H.; Abuelo, D.; Dietz, H. C.; Basson, C. T.; Shete, S. S.; Milewicz, D. M. Familial thoracic aortic aneurysms and dissections: genetic heterogeneity with a major locus mapping to 5q13−14. *Circulation* **2001**, *103* (20), 2461−2468.

(14) Inamoto, S.; Kwartler, C. S.; Lafont, A. L.; Liang, Y. Y.; Fadulu, V. T.; Duraisamy, S.; Willing, M.; Estrera, A.; Safi, H.; Hannibal, M. C.; Carey, J.; Wiktorowicz, J.; Tan, F. K.; Feng, X. H.; Pannu, H.; Milewicz, D. M. TGFBR2 mutations alter smooth muscle cell phenotype and predispose to thoracic aortic aneurysms and dissections. *Cardiovasc. Res.* **2010**, *88*, 520−529.

(15) Tyers, M.; Mann, M. From genomics to proteomics. *Nature* **2003**, *422* (6928), 193−197.

(16) Yates, J. R., III. Mass spectrometry: from genomics to proteomics. *Trends Genet.* **2000**, *16* (1), 5−8.

(17) Azuaje, F.; Devaux, Y.; Wagner, D. Computational biology for cardiovascular biomarker discovery. *Briefings Bioinf.* **2009**, *10* (4), 367−377.

(18) Old, W. M.; Meyer-Arendt, K.; Aveline-Wolf, L.; Pierce, K. G.; Mendoza, A.; Sevinsky, J. R.; Resing, K. A.; Ahn, N. G. Comparison of label-free methods for quantifying human proteins by shotgun proteomics. *Mol. Cell. Proteomics* **2005**, *4* (10), 1487−1502.

(19) Zhu, W.; Smith, J. W.; Huang, C.-M., Mass spectrometry-based label-free quantitative proteomics. *BioMed Res. Int.* **2009**, *2010*.

(20) Aebersold, R.; Mann, M. Mass spectrometry-based proteomics. *Nature* **2003**, *422* (6928), 198−207.

(21) Liao, M.; Liu, Z.; Bao, J.; Zhao, Z.; Hu, J.; Feng, X.; Feng, R.; Lu, Q.; Mei, Z.; Liu, Y.; Wu, Q.; Jing, Z. A proteomic study of the aortic media in human thoracic aortic dissection: implication for oxidative stress. *J. Thoracic Cardiovasc. Surg.* **2008**, *136* (1), 65−72.e3.

(22) Farina, A.; Chambery, A.; Esposito, S.; Agozzino, L.; Cotrufo, M.; Della Corte, A.; Parente, A. Proteomic profiling of medial degeneration in human ascending aorta. *Clin. Biochem.* **2010**, *43* (4−5), 387−396.

(23) Pilop, C.; Aregger, F.; Gorman, R. C.; Brunisholz, R.; Gerrits, B.; Schaffner, T.; Gorman, J. H., 3rd; Matyas, G.; Carrel, T.; Frey, B. M. Proteomic analysis in aortic media of patients with Marfan syndrome reveals increased activity of calpain 2 in aortic aneurysms. *Circulation* **2009**, *120* (11), 983−991.

(24) Abdulkareem, N.; Skroblin, P.; Jahangiri, M.; Mayr, M. Proteomics in aortic aneurysm−What have we learnt so far? *Proteomics: Clin. Appl.* **2013**, *7* (7−8), 504−515.

(25) Ladanyi, A.; Sipos, F.; Szoke, D.; Galamb, O.; Molnar, B.; Tulassay, Z. Laser microdissection in translational and clinical research. *Cytometry, Part A* **2006**, *69* (9), 947−960.
(26) von Eggeling, F.; Melle, C.; Ernst, G. Microdissecting the proteome. *Proteomics* **2007**, *7* (16), 2729−2737.
(27) Espina, V.; Wulfkuhle, J. D.; Calvert, V. S.; VanMeter, A.; Zhou, W.; Coukos, G.; Geho, D. H.; Petricoin, E. F., 3rd; Liotta, L. A. Laser-capture microdissection. *Nat. Protoc.* **2006**, *1* (2), 586−603.
(28) Wisniewski, J. R.; Zougman, A.; Nagaraj, N.; Mann, M. Universal sample preparation method for proteome analysis. *Nat. Methods* **2009**, *6* (5), 359.
(29) Tang, Z.; Baykal, A. T.; Gao, H.; Quezada, H. C.; Zhang, H.; Bereczki, E.; Serhatli, M.; Baykal, B.; Acioglu, C.; Wang, S. mTor Is a Signaling Hub in Cell Survival: A Mass-Spectrometry-Based Proteomics Investigation. *J. Proteome Res.* **2014**, *13* (5), 2433−2444.
(30) Yang, J.; Maity, B.; Huang, J.; Gao, Z.; Stewart, A.; Weiss, R. M.; Anderson, M. E.; Fisher, R. A. G-protein inactivator RGS6 mediates myocardial cell apoptosis and cardiomyopathy caused by doxorubicin. *Cancer Res.* **2013**, *73* (6), 1662−1667.
(31) Didangelos, A.; Yin, X.; Mandal, K.; Saje, A.; Smith, A.; Xu, Q.; Jahangiri, M.; Mayr, M. Extracellular matrix composition and remodeling in human abdominal aortic aneurysms: a proteomics approach. *Mol. Cell. Proteomics* **2011**, *10* (8), M111.008128.
(32) Beamish, J. A.; He, P.; Kottke-Marchant, K.; Marchant, R. E. Molecular regulation of contractile smooth muscle cell phenotype: implications for vascular tissue engineering. *Tissue Eng., Part B* **2010**, *16* (5), 467−491.
(33) Owens, G. K.; Kumar, M. S.; Wamhoff, B. R. Molecular regulation of vascular smooth muscle cell differentiation in development and disease. *Physiol. Rev.* **2004**, *84* (3), 767−801.
(34) Kumar, M. S.; Owens, G. K. Combinatorial control of smooth muscle-specific gene expression. *Arterioscler., Thromb., Vasc. Biol.* **2003**, *23* (5), 737−747.
(35) Ailawadi, G.; Moehle, C. W.; Pei, H.; Walton, S. P.; Yang, Z.; Kron, I. L.; Lau, C. L.; Owens, G. K. Smooth muscle phenotypic modulation is an early event in aortic aneurysms. *J. Thorac. Cardiovasc. Surg.* **2009**, *138* (6), 1392−1399.
(36) Zou, S.; Ren, P.; Nguyen, M.; Coselli, J. S.; Shen, Y. H.; LeMaire, S. A. Notch signaling in descending thoracic aortic aneurysm and dissection. *PLoS One* **2012**, *7* (12), e52833.
(37) Kjellqvist, S.; Maleki, S.; Olsson, T.; Chwastyniak, M.; Branca, R. M.; Lehtio, J.; Pinet, F.; Franco-Cereceda, A.; Eriksson, P. A combined proteomic and transcriptomic approach shows diverging molecular mechanisms in thoracic aortic aneurysm development in patients with tricuspid- and bicuspid aortic valve. *Mol. Cell. Proteomics* **2013**, *12* (2), 407−425.
(38) Elefteriades, J. A. Thoracic Aortic Aneurysm: Reading the Enemy's Playbook. *Yale J. Biol. Med.* **2008**, *81*, 175−186.
(39) Zhu, L.; Vranckx, R.; Van Kien, P. K.; Lalande, A.; Boisset, N.; Mathieu, F.; Wegman, M.; Glancy, L.; Gasc, J.-M.; Brunotte, F. Mutations in myosin heavy chain 11 cause a syndrome associating thoracic aortic aneurysm/aortic dissection and patent ductus arteriosus. *Nat. Genet.* **2006**, *38* (3), 343−349.
(40) Jones, J. A.; Zavadzkas, J. A.; Chang, E. I.; Sheats, N.; Koval, C.; Stroud, R. E.; Spinale, F. G.; Ikonomidis, J. S. Cellular phenotype transformation occurs during thoracic aortic aneurysm development. *J. Thorac. Cardiovasc. Surg.* **2010**, *140* (3), 653−659.
(41) JOnes, J. A.; Beck, C.; Barbour, J. R.; Zavadzkas, J. A.; Mukherjee, R.; Spinale, F. G.; Ikonomidis, J. S. Alterations in Aortic Cellular Constituents during Thoracic Aortic Aneurysm Development. *Am. J. Pathol.* **2009**, *175* (4), 1746−1756.
(42) Moxon, J. V.; Padula, M. P.; Clancy, P.; Emeto, T. I.; Herbert, B. R.; Norman, P. E.; Golledge, J. Proteomic analysis of intra-arterial thrombus secretions reveals a negative. *Atherosclerosis* **2011**, *219* (2), 432−439.
(43) Sariola, H.; Viljanen, T.; Luosto, R. Histological pattern and changes in extracellular matrix in aortic dissections. *J. Clin. Pathol.* **1986**, *39* (10), 1074−1081.
(44) Matsumoto, K.; Maniwa, T.; Tanaka, T.; Satoh, K.; Okunishi, H.; Oda, T. Proteomic analysis of calcified abdominal and thoracic aortic aneurysms. *Int. J. Mol. Med.* **2012**, *30* (2), 417−429.
(45) Taketani, T.; Imai, Y.; Morota, T.; Maemura, K.; Morita, H.; Hayashi, D.; Yamazaki, T.; Nagai, R.; Takamoto, S. Altered patterns of gene expression specific to thoracic aortic aneurysms. *Int. Heart J.* **2005**, *46* (2), 265−277.
(46) Henn, D.; Bandner-Risch, D.; Perttunen, H.; Schmied, W.; Porras, C.; Ceballos, F.; Rodriguez-Losada, N.; Schäfers, H. Identification of Reference Genes for Quantitative RT-PCR in Ascending Aortic Aneurysms. *PLoS One* **2013**, *8* (1), e54132.
(47) Basu, R.; Fan, D.; Kandalam, V.; Lee, J.; Das, S. K.; Wang, X.; Baldwin, T. A.; Oudit, G. Y.; Kassiri, Z. Loss of Timp3 gene leads to abdominal aortic aneurysm formation in response to angiotensin II. *J. Biol. Chem.* **2012**, *287* (53), 44083−44096.
(48) Modrego, J.; Lopez-Farre, A. J.; Martinez-Lopez, I.; Muela, M.; Macaya, C.; Serrano, J.; Monux, G. Expression of cytoskeleton and energetic metabolism-related proteins at human abdominal aortic aneurysm sites. *J. Vasc. Surg.* **2012**, *55* (4), 1124−1133.
(49) Arcucci, A.; Ruocco, M. R.; Albano, F.; Romano, V.; Granato, G.; De Vendittis, E.; Della Corte, A.; Bancone, C.; Montagnani, S. Analysis of SOD3 and Akt in ascending aortic aneurysm. *Ital. J. Anat. Embryol.* **2013**, *118* (2), 16.
(50) Acosta-Martin, A. E.; Panchaud, A.; Chwastyniak, M.; Dupont, A.; Juthier, F.; Gautier, C.; Jude, B.; Amouyel, P.; Goodlett, D. R.; Pinet, F. Quantitative Mass Spectrometry Analysis Using PAcIFIC for the Identification of Plasma Diagnostic Biomarkers for Abdominal Aortic Aneurysm. *PLoS One* **2011**, *6* (12), e28698.